PERSPECTIVE   OPEN

Searching for new ferroelectrics and multiferroics: A user's point of view

JF Scott[1]

A perspective on computational studies of ferroelectrics and multiferroics is given that emphasises what has yet to be done, along with some subtleties in previously studied systems. Beginning with the extensive data-mining studies of Abrahams and more recently, Rabe, a survey is given of magnetostrictive effects in antiferromagnetic antiferroelectrics (after Toledano and Toledano), which has an nonmagnetic analogy in the antiferroelectric phase of tris-sarcosine calcium chloride and a reminder of the unusual spin–phonon coupling of Holden *et al.* in systems such as $KCoF_3$ and $EuTiO_3$. Attention is also paid to field-temperature phase diagrams, finite non-periodic boundary conditions, and processing-dependent structures.

INTRODUCTION

The search for new ferroelectrics has been proceeding in at least three different ways: (1) data mining of existing crystallographic data;[1] (2) ab initio calculations, particularly by density functional theory (DFT) of new families;[2] (3) new techniques of fabrication, including high-pressure synthesis or infiltration of the gaps between surfaces.[3] In the present paper I address qualitatively some subtleties that might help guide these efforts, not from the technical calculation point of view, but as an interested observer and user of such predictions wishing to fabricate new device embodiments.

ABRAHAMS' CRITERION

In a lengthy series of papers Sidney Abrahams, formerly head of the crystallography department at Bell Labs and president of the American Crystallography Society, presented a thorough review of materials that had a good but unproven probability of being ferroelectrics.[4–6] Abrahams had a specific criterion for these choices: The ionic positions must be off-centred (acentric symmetry) but within small specified distances from being centred. We can express his criterion as

$$0 < r < 0.01 \text{ nm} \tag{1}$$

where r is the distance from a centred position for the ion in question; the upper limit in Equation (1) is rather arbitrary but intended to be $\ll$ the bond length for the ion to nearest neighbour(s) and hence, compatible with switching with a modest coercive field (less than the breakdown field).

Using this criterion Abrahams predicted a large number of new ferroelectrics, and a significant number of these were later shown to be ferroelectric.[7,8]

Another example, discussed below, is β-Na_2UF_6, which has been published by the same author[9,10] as both paraelectric P6_2m and acentric ferroelectric P32_1. Heavy twinning has prevented a definitive structural analysis.[11] In general, twinning has often prevented definitive structural studies (e.g., famously in $SrTiO_3$ and $LaAlO_3$).

CRYSTALLOGRAPHERS' PROTOCOL

One of the problems arising with data mining is that researchers do not always recognise the most important protocol in crystallographic structural reports: The symmetry published must be the highest compatible with the highest point group symmetry for each ion that is possible within experimental uncertainty. This means that structures are often reported with centred phases whereas, their ions, particularly the lighter ions such as O, F, and H, are probably off-centred. Until the advent of modern synchrotron sources, this was such a serious problem that structures of even simple lattices such as perovskites ($SrTiO_3$, $LaAlO_3$ and $PrAlO_3$)[12–14] were incorrect (corrected by Raman techniques,[15–17]) and the positions of H in hydrogen-bonded ferroelectrics was complete guesswork. My estimate is that at least 10% of the structures published in Wycoff are lower in reality, including many ferroelectrics. Paradoxically these include those slightly acentric materials most likely to exhibit ferroelectric switching.

ACTINIDES—THE 'ACID TEST' FOR DFT

Actinide fluorides

Density functional calculations have trouble with d-electrons and so they have much more trouble with 5f states. That is a pity, because the actinides (excluding thorium) are multiferroic and very interesting. We have already alluded above to the interest in Na_2UF_6, but there are many other actinide fluorides that might be ferroelectric, including hexagonal C32 $NaPuF_4$ and Na_3UF_6, with octyfluorides such as PuOF and UOF having pseudocubic rhombohedral and tetragonal phases, whereas AcOF is truly cubic.[18] The latter sequence would be a good challenge to DFT theory, particularly to show why AcOF is cubic and PuOF and UOF noncubic.

Rather recently (2015) Jason Lashley (unpublished) at Los Alamos has shown that UO_2 is probably noncubic (tetragonal) at modest temperatures below ambient. Strong phonon–magnon coupling is well known[19,20] in UO_2.

[1]School of Chemistry and School of Physics, St Andrews University, St Andrews, Fife, Scotland.
Correspondence: JF Scott (jfs4@st-andrews.ac.uk)

Other oxyfluorides

French and Russian groups have shown that systems such as NH_4FePO_4F (acentric $Pna2_1$ to $Pnma$) are probably[21] not only ferroelectric but multiferroic; and both elpasolites (e.g., $K_3MoO_3F_3$ or $(NH_3)_3TiOF_3$) and chiolites (e.g., $Na_4Lu(WNb_2)O_9F$) merit further study.

ANTIFERROMAGNETIC ANTIFERROELECTRICS

Whenever two adjacent spins order antiparallel, magnetostriction effects are likely to cause those ions to move closer together or farther apart. Thus, in principle, most antiferromagnets also double their primitive chemical unit cell below T(Neel); however, this effect is usually negligible and ignored. In some cases this antiferromagnetic order does change the structure, and a structural phase transition occurs.[22] Toledano and Toledano[23,24] have discussed the case of a magnetically induced phase transition from $Pca2_1'$ (the nickel chlorine boracite structure) to $P2_1$, using Landau free energies.

Kornetzki; Toledano and Toledano

Starting with the free energy of form

$$F_m = F_o + \Sigma(a_i/2)L_i^2 + (c/2)M^2 + \Sigma b_i L_i^4 + (d/4)M^4$$
$$+ (v_{1z}/2)L_i z^2 + (v^{2z}/2)L_2 z^2 + (v_3/2)L_{3z}^2$$
$$+ (b_z/2)M_z^2 \tag{2}$$

where L and M are defined as

$$M = \mu_1 + \mu_2 + \mu_3 + \mu_4$$
$$L_1 = \mu_1 - \mu_2 + \mu_3 - \mu_4$$
$$L_2 = \mu_1 + \mu_2 - \mu_3 - \mu_4 \tag{3}$$
$$L_3 = \mu_1 - \mu_2 - \mu_3 + \mu_4$$

for magnetic moments μ on four spin sites 1, 2, 3 and 4.

The magnetoelastic free energy is

$$F_{ME} = \delta_1 L_1 z^2 e_{xz} + \delta_2 L_{2z}^2 e_{xy} + (\delta_3 e_{xx} + \delta_4 e_{yy} + \delta_5 e_{zz})L_{3z}^2$$
$$+ \delta_6 M_z^2 e_{yz}. \tag{4}$$

And the elastic terms

$$F_E = \frac{1}{2}(C_{11}e_{xx}^2 + C_{22}e_{yy}^2 + C_{33}e_{zz}^2) + C_{12}e_{xy}^2 + C_{13}e_{xz}^2$$
$$+ C_{23}e_{yz}^2. \tag{5}$$

They show that this permits two types of ordering of relativistic origin: (1) an induced magnetization

$$M_z = -(a_2/\sigma_2)L_{2x} \tag{6}$$

corresponding to weak ferromagnetism along z (here σ terms couple L to M), and

$$\text{canting angle} = \tan(-a_2/\sigma_2) = M_z/L_{2x}; \tag{7}$$

and also: (2) an induced antiferromagnetic order along the y axis given by

$$L_{2y} = (-a_2/\delta_4)L_{2x}. \tag{8}$$

Here δ relates strain: e.g., $e_{xz} = (-\delta_1/C_{13}) L_{1z}^2$ and so on.

The full free energy also includes the elastic terms

$$F_E = \frac{1}{2}\big[(C_{11}e_{xx}^2 + C_{22}e_{yy}^2 + C_{33}e_{zz}^2) + C_{12}e_{xy}^2 + C_{13}e_{xz}^2 + C_{23}e_{yz}^2\big] \tag{9}$$

And the minimisation of the full free energy gives three different possible structures:

(i) If the coefficient c vanishes first at the Neel transition, a spontaneous strain

$$e_{yz} = -(\delta_6/C_{23})M_z^2 \tag{10}$$

occurs, leading to a structural phase transition to $Pc'a'2_1$;

(ii) If a_1 vanishes first, the strain is

$$e_{xz} = -(\delta_1/C_{13})L_{1z}^2 \tag{11}$$

leading to a monoclinic $Pb(y)$ structure.

(iii) If a_2 vanishes first, the phase change is to $Pc'a2_1'$.

(iv) And if a_3 changes at T(N), no structural phase transition occurs.

That is, a structural phase transition does NOT always occur. In this case a volumetric magnetostriction occurs.[21] Volume magnetostriction has been understood for about 80 years but still has new wrinkles.[22]

EuTiO$_3$ and the Buyers–Cowley model of antiferromagnetic structural effects

In 1971 Holden et al.[25] developed a model applicable to magnetic perovskites such as $KCoF_3$ in which a rotational instability in the antiferrodistortive soft mode like that in $SrTiO_3$ or $LaAlO_3$ occurs. In addition to the magnetostrictive effects discussed above, such a system has a more direct coupling between vibrations and magnetic spins and hence between magnetic ordering and structural phase transitions. They point out that the soft mode involving oxygen octahedral rotation carries with it an orbital angular momentum; and this momentum can couple directly to the spins at the A or B sites. This spin–orbit coupling will be in addition to and may be larger than magnetostriction. It is expected to be unusually large in systems such as Co^{++} with large unquenched orbital angular momenta. It results in extra lines in the perovskite Raman spectra below T(Neel) in $KCoF_3$, $RbCoF_3$ and $TlCoF_3$,[26–29] and probably in the planar magnets K_2CoF_4, Tl_2CoF_4 and so on.[30] Most important in the present-day context, it should also occur in $EuTiO_3$, where the antiferrodistortive transition[31,32] occurs near 282 K. Note that since this is an antiferrodistortive transition, the soft optic phonon is at the Brillouin zone boundary (critical point R at the [111] corner); although magnon-like spin waves do not exist as propagating modes at T ≫ T(Neel) for very long wavelengths at the Brillouin zone centre, they still exist for very short wavelengths at the zone boundary and can therefore couple to phonons.

Holden et al. and Scott et al.[25,26] find a spin–lattice interaction energy of $c = 9 \pm 2$ cm^{-1} experimentally and 12 cm^{-1} theoretically, compatible with a lattice distortion from Gladney (40) of $\delta a/a = 0.2\%$ along the a axis. The key equation is of form

$$C = (-6/35)(Z_f e^2/R^3)(\delta a/a)<r^2>(ak_{orb})^2 \tag{12}$$

where $-Z_f e$ is the fluorine ion charge; $<r^2>$ is the mean radius of the 3d electron in Angstroms squared; other terms defined elsewhere.[25]

It is also useful to be reminded that in all titanates entropy requires that there are some oxygen vacancies. Ti^{+4} ions near such vacancies convert to Ti^{+3}, which is a magnetic ion. Therefore titanates, especially in regions near domain walls (which trap oxygen vacancies) may exhibit unexpected magnetoelectric effects in substances such as $SrTiO_3$ that nominally lack magnetic ions.

SPATIAL AND TEMPORAL COHERENCE: ENERGY LANDSCAPES

An important concern, in addition to symmetry differences related to processing procedures, is the fact that many chemical compounds have numerous symmetry-unrelated phases with ground state energies only a few meV apart. SiO_2 is probably the most notorious of these, with various quartz structures, plus
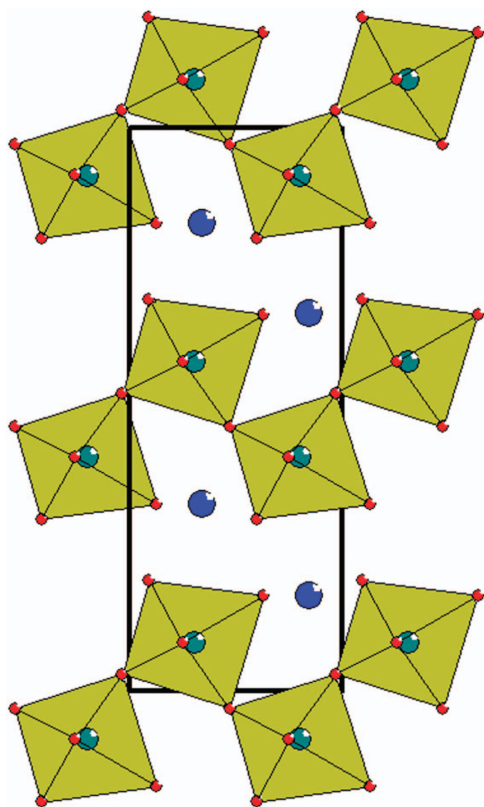
Figure 1. Structure of topological ferroelectric $LaTaO_4$.

cristobalites, tridymites, coesite, stishovite and so on. These are of great importance to mineralogists and geologists, and yet in some cases controversies remain over many decades until the present. β-cristobalite is a notorious example, with Dove et al. publishing several papers[33,34] that maintain it is cubic, yet the ab initio calculation of Coh and Vanderbilt showing[35] that to be incorrect; and both infrared and Raman studies of the present author[36] confirming Vanderbilt's theory. Isomorphs such as cristobalite $AlPO_4$ have the same phase transition exhibiting non-subgroup symmetry relationship to the parent phase; the symmetries in each case are lower than in SiO_2, due to inequivalent Al and P ions, but the argument is the same.

β-cristobalite

The problem with cristobalite is that its α and β phases do not satisfy a subgroup–group relationship. Hence, the phase transition is first order and technically 'reconstructive,'[37] yet it exhibits a soft optical vibrational mode similar to those in second-order displacive systems. The problem seems to be spatial and temporal coherence. Dove et al. has maintained adamantly that the structure is cubic and disordered on a length scale of a few atoms or unit cells; but he does not specify his time scale. Conventional non-synchrotron sources generally give X-ray information on the time scale of seconds. Yet crystal structures can be well-defined and carry out many physical processes (absorption and emission of light) on time scales of picosecond or less. Thus, it is not particularly useful for physicists, unlike geologists, to be told that cristobalite is cubic on a time scale of seconds or minutes. These criteria of correlation lengths and times are usually unspecified in DFT calculations, and of course will be highly temperature dependent. In β-cristobalite it is quite certain that the structure is not cubic with ions at inversion centres, since that would produce no first-order Raman spectra (all vibrations of odd parity), whereas experiments reveal three strong Raman lines.

Moreover, although the non-cubic structure may average out over long times of interest to mineralogists, they do not over times adequate to emit and absorb light or carry out electronic transitions, which is a reasonable definition of a stable phase for physicists.

The moral in this story is that care must be exercised in looking for crystal symmetry at phase transitions, and nearly continuous (no fracture of crystals) need not imply subgroup relations. Energy landscapes are often filled with ground states very close together (meV), and the experimental phase sequence can miss subgroup transitions in favour of 'sibling' phases descended from the same parent phase but not satisfying group-subgroup criteria, even when such paths exist. Furthermore, the coherence times and lengths for such ground states are usually undetermined via DFT calculations.

$LaTaO_4$ and $LaNbO_4$

$LaTaO_4$, $LaNbO_4$ and their lanthanide rare earth isomorphs are isostructural with $BaMnF_4$, $BaNiF_4$ and so on, with structure shown in Figure 1. These are 'geometric ferroelectrics' with planar structures and magnetoelectric effects.[38–41] In addition to the $A2_1am$ orthorhombic structures of $BaMnF_4$, the oxides also have a different ferroelastic structure with 2/m–4/m symmetry change at a ferroelastic transition.[42] It is not known whether the 2/m ferroelastic centric structure is a lower-energy state than the ferroelectric $A2_1am$ state. This family of materials, both fluorides and oxides, are of practical importance in another context: $SrMgF_4$ is the ferroelectric with the largest bandgap in nature; at $E_g = 12.50$ eV it can be used for second harmonic generation from 2,000–1,000 Å.[43] The oxyfluorides of this family have not been explored, and it is not known if any are stable in this structure.

STRUCTURE VIA PROCESSING

It often happens that the structure of oxides is strongly dependent on their processing conditions, particularly the annealing cycle. The most notorious and best-studied example is lead scandium tantalate, $PbSc_{1/2}Ta_{1/2}O_3$, often abbreviated as PST. This useful relaxor ferroelectric can be prepared with Sc and Ta ions at the B sites almost perfectly ordered or alternatively, completely randomly disordered, depending only on the annealing procedure. In fact, not only are the phases different in symmetry, but even the number of phases stable at different temperatures is not the same and can include incommensurate phases. The situations in $PbFe_{1/2}Nb_{1/2}O_3$ (PFN) and $PbFe_{1/2}Ta_{1/2}O_3$ (PFT) may be similar.

PST

At present the conventional wisdom is that PST somewhere above $T_c = 299$ K is that it has Fm3m cubic structure with ordered Sc and Ta ions giving a doubled perovskite primitive cell (PFN and PFT have the same Fm3m structure)[44–49]. For a fully disordered material, the average structure is Pm3m. Setter and Cross concluded that at 299 K there is a single paraelectric–ferroelectric transition to a rhombohedral structure. However, Salje et al. showed[45] that most samples exhibit a two-step ferroelectric transition from Fm3m to R3_c to R3c; and others have shown that this Pm3m structure is reached only above $T = 723$ K, and that between 300 and 700 K several additional phases exist, including an orthorhombic $C222_1$ phase similar to that in $Pb(Mg,W)O_3$; and at least one incommensurate phase exists between 299 and 323 K, depending on annealing cycles. These situations are reviewed in refs 48,49.

$InMnO_3$

Similar to PST, indium manganite can be in a ferroelectric $P6_3cm$ state at low temperatures[48] or a non-ferroelectric P3_c1 symmetry
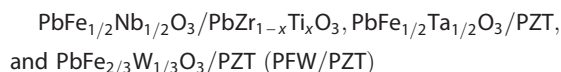
4

state.[48–50] The latter can be quenched at room temperature. The work of Spaldin and Fiebig is quite beautiful and theory and experiment agree, with full pole figures; but as Cheong's group has shown[49], those measurements were on a metastable state quenched to ambient,[50] and not on the true ground state.

Room temperature multiferroic GaFeO$_3$

Gallium orthoferrite is a room temperature multiferroic whose properties have been controversial due to processing. Very detailed studies of its ferroelectric switching in bulk were published by Garg's group in India;[51,52] with earlier work in China,[53] but these disagreed qualitatively with the thin-film data from Pohang.[54] Very recently this year this has been reconciled,[54] with o-GaFeO$_3$ demonstrating good ferroelectric switching in thin films 50–200 nm thick up to 405 K, above which leakage currents become unacceptably large; this satisfies most commercial and military specifications for a memory material. The differences arise in part from the processing conditions for sol-gel films compared with single-crystal samples. The structure is ferromagnetic, with Fe +3 ions at different sites yielding a net magnetization of 0.3 Bohr magnetons per unit cell at low temperatures, significantly better than BiFeO$_3$. The material has strong magnetoelectric effects at ambient temperatures and exhibits Vogel–Fulcher relaxation for both its magnetization near T(Neel) and its polarisation. This glassy behaviour arises from Ga ions at Fe sites and vice versa (same valence and size).

MULTI-ION B-SITE OCCUPANCY SYSTEMS

A particular topic of current interest[55–59] is room temperature multiferroic materials with four different ions at the perovskite B site (Ti, Zr, Fe and either Ta or Nb), such as $Pb(Fe_{1/2}Nb_{1/2})_{1-y}[Ti_{0.53}Zr_{0.47}]_yO_3$. These require too large a cell for present DFT calculations, although V. Cooper (private communication) is beginning the three-ion B-site case of $Pb(Fe_{1/2}Nb_{1/2})_{1-y}Ti_yO_3$ (a single-phase mixture of PbTiO$_3$ and PFN).

$$PbFe_{1/2}Nb_{1/2}O_3/PbZr_{1-x}Ti_xO_3, PbFe_{1/2}Ta_{1/2}O_3/PZT,$$

$$and\ PbFe_{2/3}W_{1/3}O_3/PZT\ (PFW/PZT)$$

This system merits considerably more computational work because it is a family of room temperature multiferroics. The magnetic field dependence of its room temperature dielectric response has very recently been modelled this year, with very good agreement with experiment.[58] The PFW/PZT single-phase material has received the least attention,[59] although it has unusual magnetic field dependence for its dielectric constant (probably due to charge injection through its electrodes, which creates an inductance even in a parallel-plate capacitor[60,61]), and a detailed indirect coupling model for polarisation and magnetization via electrostriction.[62,63]

FINITE SYSTEMS

The ab initio calculations such as DFT normally employ cylindrical periodic boundary conditions. However, growing evidence indicates that the stability of phases may hinge critically on the assumed boundary conditions. This is especially clear in switching of domains,[64–66] but it also applies to phase stability, with thin films of e.g., BaTiO$_3$ or Ba$_{1-x}$Sr$_x$TiO$_3$ exhibiting Tc several hundred degrees higher than in bulk.[67,68] Thus, finite geometry should be considered in computational studies.

Infiltration systems (Noheda)

A particularly elegant system is that in which a phase of TbMnO$_3$ grows nicely[3] as it infiltrates narrow slots between other materials, such as SrTiO$_3$, where it grows under stress. This result was first presented in 2013 but misinterpreted as stacking faults. It was correctly interpreted at its presentation by the present author. It is of potentially great importance in device processing. Moreover, starting with the seminal work on SrTiO$_3$/LaAlO$_3$ interfaces, it is clear that SrTiO$_3$ surfaces in particular play a strong role in enhancing superconductivity, even in pnictides. Interfaces and boundary conditions are not minor perturbations in phase stability.

Other finite-size systems: Bessel function structures (Gruverman; Baudry and Lukyanchuk and Sene)

There are finite-size systems of other geometries that merit attention: Thin-film nano-discs are frequently studied and exhibit very unusual nucleation and growth of phases with applied switching fields[69,70] and temperature changes, displaying Bessel-function spatial patterns[71,72] and unpredicted polygonal faceting,[73] probably due to surface tension. These phases need not be stable in samples of infinite or periodic lateral boundary conditions (Figure 2).

Cylinder stress systems (Lichtensteiger and Triscone; Scott)

In nanostructures, particularly in nano discs, the boundary conditions also involve cylinder stress (or 'hoop stress'). This
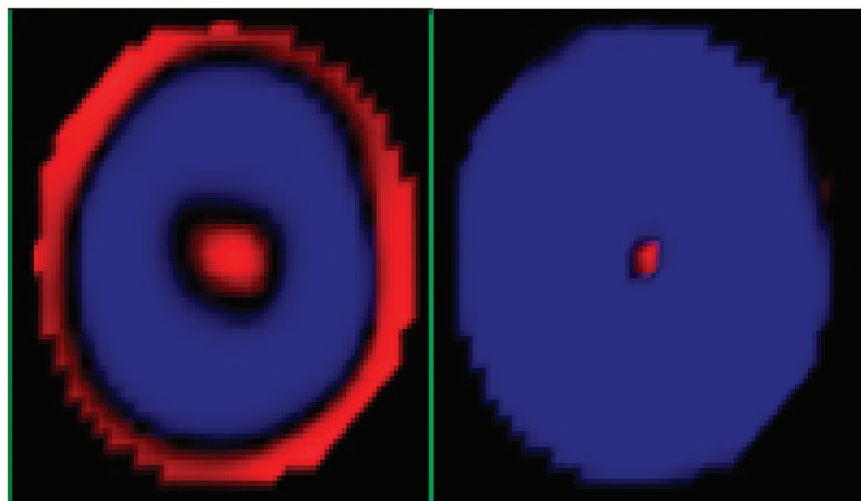

Figure 2. +P and − P circular domains in a 1-micron diameter PZT thin-film disk, showing Bessel-function type geometries.

effect can be large and should not be neglected in calculating phase stability.[74,75]

Artificial superlattices (Dawber; Zubko; Jiang, Rios and Scott)

Of course the most obvious case of finite geometries and their relationship to phase stability is in the area of artificial superlattices. Fortunately these have been reviewed carefully elsewhere.[76]

It is worth pointing out, however, the work of Jiang et al.[67] and Rabe's group[68] on $BaTiO_3/SrTiO_3$ superlattices, since they are highly counter-intuitive. When barium titanate and strontium titanate are stacked as superlattices, it is not surprising that the barium titanate [001] polarisation polarises the adjacent nonpolar $SrTiO_3$ blocks; it is very surprising, however, that the latter is along [110]. This arises in relaxed structures and is despite the fact that Poisson's Law creates an energetically costly interfacial electrostatic energy; that is overcompensated by reduced strain energy.

QUANTUM CRITICAL POINTS: O^{18} $SrTiO_3$, TSCC:Br, $PbFe_3Ga_9O_{19}$, $BaFe_3Al_9O_{19}$

Predicting ferroelectric structures may be hard enough for computational physicists, but it should in some sense be easier for quantum critical point systems, since their Curie or Neel temperatures are at or very near $T = 0$. Nevertheless, not much has yet been published. The following eight ferroelectric QCP systems have been studied experimentally:

$SrTiO_3$ (^{18}O, ^{16}O and mixed, with 38% ^{18}O being closest to $T_c = 0$);[77] $KTaO_3$;[77] tris-sarcosine calcium chloride with Br;[78] $BaFe_{12}O_{19}$,[79] $SrFe_{12}O_{19}$,[79] and $PbFe_{2-x}Ga_xO19$.[79] The last cited has a magnetic quantum critical point at $x = 9$. Ironically, all are second-order displacive phase transitions, whereas some very good theoreticians have predicted that they must be first order and order–disorder.[80] The hexaferrites are p-type semiconductors with bandgaps between 1 and 2 eV, and they are Lieb–Mattis antiferromagnets with very large net ferromagnetic moments, with 16 Fe^{+3} spins up and 8 Fe^{+3} spins down in the $Z = 2$ primitive unit cell. With 58 ions per unit cell, they are slightly too large for most present-day DFT calculations (see however refs 81,82).

The hexaferrites satisfy the 1970 prediction of Shneerson et al.[81,82] that reciprocal dielectric constant varies near $T = 0$ as T^3, and the temperature regime of criticality is found to be ca. 15 K for $BaFe_{12}O_{19}$ and 30 K for $SrFe_{12}O_{19}$.

TOPOLOGICAL DEFECT SYSTEMS—SKYRMION MODELS: ZAKRZEWSKI; GRUVERMAN AND SCOTT; RAMESH

An additional complication in computational structures for ferroelectrics is that they exhibit topologically singular arrays of skyrmions: Fu and Bellaiche;[83] Borisevich;[84] and Ramesh et al.[85] These resemble Abrikosov vortex arrays in Type-II superconductors, but they have not yet been computationally modelled.

Skyrmions in magnets and ferroelectrics were considered by Zakrewski et al.[86] and by Dawber et al.[87]

INCOMMENSURATE STRUCTURE PREDICTIONS

The incommensurate material[88–92] of maximum multiferroic interest is probably $BaMnF_4$.[39,40] Whereas Ederer et al.[41] did a nice DFT computation for $BaNiF_4$, the situation in $BaMnF_4$ is far more challenging, because it has incommensurate phases between its paraelectric and ferroelectric phase. Samples from Howard Guggenheim at Bell Labs were used in both the work at Brookhaven[88,92] (Eibschutz et al.) and by the present author. These exhibit a single paraelectric–ferroelectric transition near 254 K with soft mode at $q* = (0.392, 1/2, 1/2)$ $a*$ of the high-temperature

phase. Unusually for incommensurates, this wave vector is independent of T down to $T = 4$ K, an effect we view as pinning by defects, probably fluorine vacancies. However, in other specimens grown in France and in Slovenia, Barthes-Regis et al.[89] and Levstik et al.[90] found two or more phase transitions from ca. 250 K down to ca. 80 K, where a ferroelectric lock-in transition occurs to a commensurate cell with five formula groups along the a axis and two orthogonal to that axis ($Z = 10$). And in fact there are at least five subtle transitions between 260 and 80 K, revealed by piezoelectric resonance (Hidaka et al.[91]), and these perhaps satisfy a Devil's staircase of critical wave vectors given by

$$qn* = (2n + 5)/(5n + 13)a*,$$ (13)

although that has not been directly confirmed. Modelling this system will be difficult. We note in passing that the final low-temperature lock-in phase to long-range ferroelectricity occurs near the temperature at which strong two-dimensional spin ordering occurs in this material, which might not be coincidental ($T_N(3d) = 27$ K; $T_N(2d) = $ ca. 80 K); in-plane magnetostriction might play a role.

The fact that the phase diagram in $BaMnF_4$ depends strongly on processing and is sample dependent is therefore analogous to the case of $InMnO_3$ or PST discussed above.

Another point of computational interest is that $BaMnF_4$ satisfies[93] the axial-next-nearest-neighbour model[94] famous for K_2SeO_4, Rb_2ZnCl_4 and so on. These systems have incommensurate structures that multiply their primitive unit cell length by large integers, and therefore describing them with Landau–Devonshire free energies requires implausible high-order terms (e.g., P^{17}), whereas the the axial-next-nearest-neighbour model does so nicely with few parameters.

The other system of multiferroic interest is the Aurivilius-phase family studied by L. Keeney et al.[95] in Cork. She found room temperature multiferroic behaviour in several of these mixed-phase ceramics, but whose chemical complexity is daunting for computational modelling.

HYDROGEN-BONDED SYSTEMS: FERROELECTRIC AND ANTIFERROELECTRIC TSCC

In recent years researchers have emphasised oxide ferroelectrics and neglected hydrogen-bonded systems, based on their robustness and applicability for devices. Yet hydrogen-bonded systems retain fascinating and subtle puzzles. A good example is afforded by tris-sarcosine calcium chloride. This material has a fully displacive paraelectric–ferroelectric transition at 130 K at ambient pressure,[96,97] (Feldkamp; Banys) and a second transition[98,99] (Jones; Lashley) at 64 K (which can also be driven at room temperature with modest hydrostatic pressure). The phase below 64 K is thought to be antiferroelectric,[100] but no direct proof has been observed (no double-loop P[E] hysteresis curves). In addition, it is certain that the primitive unit cell ($Z = 4$ formula groups and 12 sarcosine molecules) does not increase below 64 K, based on new Raman data (S. Sahoo and J. S. Young, private communication). Usually antiferroelectricity involves a doubling of the ferroelectric-phase primitive unit cell, but this is not required; because TSCC has four formula groups per unit cell in its ferroelectric and paraelectric phases, it is possible that the four local polarisations simply realign in the proposed AFE phase. This does not double the number of Raman lines, but it does produce a few distinct vibrational mode frequency shifts. There are also one or two (closely spaced) phase transitions near 46 K. Since this system exhibits a quantum critical point, some modelling is warranted. However, its structure of four units of $(CH_3NHCH_2COOH)_3.2CaCl_2$ (252 atoms) makes DFT difficult, not because of the size per se, but because of the numerous H-ions and hydrogen bonds.

Thus, the four polarisations (one for each formula group) P in TSCC can reorient in a way similar to the four magnetisations at

the four spin sites in the example from Toledano and Toledano discussed in the section above on magnetostriction; that is, it is probably a ferrielectric, where four local polarisations Pi play the role of the four local magnetisations m in Equation (3) above. However, this has been neither confirmed directly by experiment nor modelled by computation.

Hydrogen-bonded ferroelectrics have other important roles in fundamental physics, with an important but often neglected series of papers by Hilczer's group[101] showing that so-called 'critical exponents' in triglycine sulphate are entirely extrinsic and can be eliminated by careful annealing and restored by irradiation. Despite her pioneering work that ruled out true fluctuation-dominated criticality, intrinsic critical exponents are still invoked by ferroelectricians every year. Note that many hydrogen-bonded systems are displacive and not order–disorder, contrary to the conventional wisdom of the 1960s.

VOLTAGE-DRIVEN MOTT TRANSITIONS: NICKELATES

The nickelates merit[102] further computational modelling to describe their phase diagram in temperature and applied electric field, since metal–insulator transitions can be driven by T or E. The latter produces an attractive memory material (metallic = ON; insulating = OFF). Since ab initio calculations now incorporate dc fields, this would seem to be a high priority task. This system is related to the (T, E) phase diagram for $NaNO_2$ discussed below:

SODIUM NITRITE: $NaNO_2$

A ferroelectric of great pedagogical value but no commercial promise is sodium nitrite, $NaNO_2$.[103,104] This simple five-atom structure consists of linear arrays of NO_2 molecules separated by Na ions. It exhibits an order–disorder phase transition in which the structure changes from (almost) all V-shaped polar NO_2 molecules in the same direction to random orientation in the paraelectric phase.

This system is notable in that it demonstrates clearly the difference between an overdamped soft mode (displacive) and a central mode due to disorder. A single vibrational normal mode, consisting of oscillation of the rigid NO_2 molecule over normal to the polar a axis, creates two peaks in the dielectric response: one is at a few hundred cm^{-1} and arises from small-amplitude motion of this mode; the other grows in intensity near T_c at frequency $f = 0$

and is due to very large amplitude flopping of the NO_2 molecule 180° from +P to − P. Note: This is an 'extra' mode not accounted for by conventional normal mode analysis, which permits three degrees of freedom per ion; such normal mode vibrational theories assume infinitesimally small amplitudes.

This system is a clear counter example to the view from others that order–disorder and displacive ferroelectric phase transitions have qualitatively similar soft-mode dynamics; we see that the former has two dielectric peak frequencies for the same normal mode coordinate, while for the latter case there is one. The existence of two peak frequencies for one normal mode is instructive for students and shows the limitations of standard group-theory determined normal mode analysis for infrared or Raman spectra near phase transformations.

In $NaNO_2$ the paraelectric phase is separated from the ferroelectric phase by a few degrees K, over which the NO_2 molecules exhibit an incommensurate modulation in angle from +a to − a.

The connection with voltage-drive phase transitions (e.g., nickelates) is that application of modest dc electric fields gives a rich phase diagram for $NaNO_2$, with for E along the polar a axis, a critical end point. Thus, in switching studies, one must be careful to keep fields low near T_c so as not to drive the system into a different structural phase and not just a different domain configuration. For ferroelectrics with an electric field along the polar axis (termed the 'conjugate field') there is in general a critical end point (as in pressure P–T diagrams in fluids), and one can go continuously from a highly polar phase to a phase with almost zero polarisation without crossing any phase boundaries. But in $NaNO_2$ with E along the polar a axis there is also a triple point (paraelectric commensurate, incommensurate, and ferroelectric) and a tricritical point at which the para- to ferroelectric transition goes from first order to second order. And if the field is applied perpendicular to the polar a axis (non-conjugate field), there is a Lifshitz point, where two phases touch tangentially
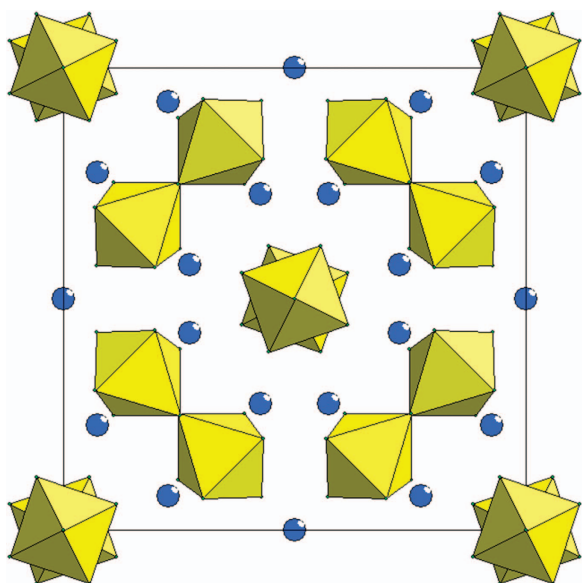

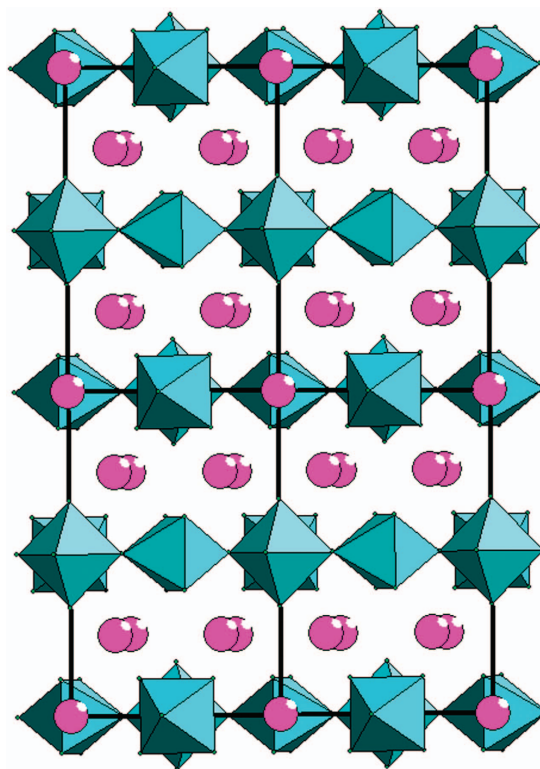**Figure 3.** Structure of $Pb_5Cr_3F_{19}$.

Figure 4. Structure of chiolites.

(more precisely, in $NaNO_2$ this Lifshitz point is not quite reached, with a first-order transition coming at a slightly lower temperature).

It would be a fine textbook example to model these phase diagrams and four different kinds of critical point (critical end point, triple point, tricritical point, and Lifshitz point) via computational methods. Parenthetically I note that Ishibashi has calculated[105] unusual critical exponents at such ferroelectric critical end points.

COMPLEX MULTIFERROICS
Three interesting families of magnetic ferroelectrics are the chiolites (Figure 3), the elpasoites, and $Pb_5Cr_3F_{19}$ (Figure 4). These are reviewed in ref. 8.

SURFACE PHASES
It is known[106–108] in $BiFeO_3$ that at least three surface phase transitions occur, including both those above ambient and below. Modelling of these via computational techniques is highly desirable, since device applications of $BiFeO_3$ are apt to emphasize thin films and surfaces.

In contrast to much other surface science work, the surface phases measured in $BiFeO_3$ do not appear to be simple $2^{1/2}$ geometric reconstructions, but they have not yet been crystallographically characterised with two-dimensional space group symmetries.

ARTEFACTS: FERROELECTRICITY IN PIG'S AORTAS, PHONON MODE SPLITTINGS DUE TO SECOND SOUND AND SO ON.
There are a lot of artefacts being published in the area of ferroelectrics and multiferroics at present.[109,110] In a way this reflects the rapidly growing interest in the field, attracting newcomers from unrelated areas on science. However, it produces a lot of papers that are obviously silly: among these are reports ferroelectricity in pig's aortas (ferroelectricity is defined in a way that requires voltage-driven switching and an acentric crystal, so it cannot occur in noncrystalline matter); or vibrational mode splitting of a doubly degenerate TA (transverse acoustic vibration) in $SrTiO_3$ interpreted as second sound. Second sound can be observed in only one or two crystals, such as NaF, where it is required that the Na and F have only one isotope. Even isotopic mixtures, let alone vacancies or defects, produce so much umklapp scattering that second sound predictions seem silly. In ferroelectrics, like all science, Okham's Razor must prevail: Don't make up far-fetched explanations for simple data; and in the case of phonon splittings, the culprit is usually a structural phase transition (tetragonal-triclinic in the case of $SrTiO_3$).[111]

SUMMARY
In summary this is not a review about computational physics from a computational physicist; instead it is a perspective addressed to computational physicists with a list of pitfalls to avoid and suggestions for future directions. I hope it is helpful in looking in the subtle areas listed. Technical points of emphasis include antiferroelectric structures in antiferromagnets and the fact that magnetostriction can induce several different structural phase changes or none at all; finite-size effects and boundary conditions; the Buyers–Cowley model of magnetoelectric coupling; and the strong dependence of phase stability upon processing (PST, $InMnO_3$ and so on).

REFERENCES
1 Bennett, J. W. & Rabe, K. M. Integration of first-principles methods and crystallographic database searches for new ferroelectrics: strategies and explorations. *J. Solid State Chem.* **195**, 21–31 (2012).

2 Bennett, J. W., Garrity, K. F., Rabe, K. M. & Vanderbilt, D. Hexagonal ABC semiconductors as ferroelectrics. *Phys. Rev. Lett.* **109**, 167602 (2012).

3 Farokhipoor, S. *et al.* Artificial chemical and magnetic structure at the domain walls of an epitaxial oxide. *Nature* **515**, 379–384 (2014).

4 Abrahams, S. C. Structurally ferroelectric $SrMgF_4$. *Acta Crystallogr. B* **58**, 34–37 (2002).

5 Abrahams, S. C. Systematic prediction of new inorganic ferroelectrics in point group 3(1) and 3(2). *Acta Crystallogr. B* **59**, 541–556 (2003).

6 Abrahams, S. C., Albertsson, J., Svensson, C. & Ravez, J. Structure of $Pb_5Cr_3F_{19}$ at 295 K, polarization reversal, and the 555 K phase transition. *Acta Crystallogr. B* **46**, 497–503 (1990).

7 Abrahams, S. C. & Ravez, J. Dielectric and related properties of fluorine-octahedra ferroelectrics. *Ferroelectrics* **135**, 21–37 (1992).

8 Scott, J. F. & Blinc, R. Multiferroic magnetoelectric fluorides. *J. Phys. Condens. Mat.* **23**, 11320 (2011).

9 Zachariasen, W. H. Crystal chemical structures of the 5f-series of elements; new structure types. *Acta Crystallogr.* **1**, 265–269 (1948).

10 Zachariasen, W. H. Double fluorides of potassium or sodium with uranium, thorium, or lanthanum. *J. Am. Chem. Soc.* **70**, 2147–2151 (1948).

11 Grzechnik, A., Fechtlekord, M., Morgenroth, W., Posse, J. M. & Friese, K. Crystal structure and stability of β-Na_2ThF_6 at non-ambient conditions. *J. Phys. Condens. Matter* **19**, 266219 (2007).

12 Lytle, F. X-ray diffractometry of low-temperature phase transformations in strontium titanate. *J. Appl. Phys.* **35**, 2212–2216 (1964).

13 Geller, S. & Bala, V. B. Crystallographic studies of perovskite-like compounds: rare earth aluminates. *Acta Crystallogr.* **9**, 1019–1025 (1956).

14 Geller, S. & Raccah, P. Phase transitions in perovskitelike compounds of rare earths. *Phys. Rev. B* **2**, 1167 (1970).

15 Fleury, P. A., Scott, J. F. & Worlock, J. M. Soft phonon modes and the 110 K phase transition in $SrTiO_3$. *Phys. Rev. Lett.* **21**, 16–19 (1968).

16 Scott, J. F. Raman study of trigonal-cubic phase transitions in rare-earth aluminates. *Phys. Rev.* **183**, 823–825 (1969).

17 Hayward, S. A. *et al.* Transformation processes in $LaAlO_3$: neutron diffraction, dielectric, thermal, optical, and Raman studies. *Phys. Rev. B* **72**, 054110 (2005).

18 Zachariasen, W. H. Crystal chemical structures of the 5f-series of elements; oxyfluorides. *Acta Crystallogr* **4**, 231–236 (1951).

19 Loiseau, T., Calage, Y., Lacorre, P. & Ferey, G. NH_4FePO_4F structural and magnetic properties. *J. Solid State Chem.* **111**, 390–396 (1994).

20 Cowley, R. A. & Dolling, G. Magnetic excitations in uranium dioxide. *Phys. Rev.* **167**, 464–477 (1968).

21 Kornetski, M. Magnetostrictions in Mn and Co, Z. *Physik* **97**, 662–666 (1935).

22 Chopra, H. D. & Wuttig, M. Non-Joulian magnetostriction. *Nature* **521**, 340–343 (2015).

23 Toledano, J. C. & Toledano, P. *Landau Theory of Phase Transitions* (World Scientific: Singapore, 1987).

24 Scott, J. F. Self-Assembly and Switching of ferroelectrics and multiferroics. *EPL* **103**, 37001 (2013).

25 Holden, T. M. *et al.* Excitations in $KCoF_3$: I. Experimental. *J. Phys. C Solid State Phys.* **4**, 2127–2138 (1971).

26 Scott, J. F. & Nouet, J. One-magnon and 2-magnon scattering in $RbCoF_3$. *Phys. Lett. A* **39**, 385–388 (1972).

27 Moch, P. & Dugautier, C. First-order phonon and magnon Raman scattering in $KCoF_3$. *Phys. Lett. A* **43**, 169–170 (1973).

28 Nouet, J., Toms, D. J. & Scott, J. F. Light scattering from magnons and excitons in RbCoF3. *Phys. Rev. B* **7**, 4874–4883 (1973).

29 Ryan, J. F., Scott, J. F. & Nouet, J. Temperature-dependent light scattering from magnetic excitons in $TlCoF_3$. *Solid State Commun.* **13**, 793–798 (1973).

30 Gesland, J. Y., Quilichini, M. & Scott, J. F. Raman spectroscopy of M_2CoF_4 planar antiferromagnets. *Solid State Commun.* **18**, 1243–1247 (1976).

31 Koehler, J., Dinnebier, R. & Bussmann-Holder, A. Structural instability of EuTiO$_3$ from x-ray powder diffraction. *Phase Trans.* **85**, 949–955 (2012).

32 Gladney, H. M. Electronic structure of MgF$_2$-Co^{++}. *Phys. Rev.* **146**, 253–260 (1966).

33 Swainson, I. P. & Dove, M. T. Low-frequency floppy modes in beta-cristobalite. *Phys. Rev. Lett.* **71**, 193–196 (1993).

34 Swainson, I. P. & Dove, M. T. 1st principles studies on structural properties of beta-cristobalite. *Phys. Rev. Lett.* **71**, 3610–3610 (1993).

35 Coh, S. & Vanderbilt, D. H. Structural stability and lattice dynamics of SiO$_2$ cristobalite. *Phys. Rev. B* **78**, 054117 (2008).

36 Zhang, M. & Scott, J. F. Raman studies of oxide minerals: a retrospective on cristobalite phases. *J. Phys. Condens. Matter* **19**, 275201 (2007).

37 Tolédano, P. & Dmitriev, V. *Reconstructive Phase Transitions: Crystals and Quasicrystals* (World Scientific: Singapore, 1996).

38 Cordrey, J. *et al.* Structure and dielectric behaviour of the topological ferroelectric La$_{1-x}$Nd$_x$TaO$_4$. *Dalton Trans.* **44**, 10673–10680 (2015).

39 Scott, J. F. Phase transitions in BaMnF$_4$. *Rep. Prog. Phys.* **42**, 1055–1084 (1979).

40 Fox, D. L., Tilley, D. R., Scott, J. F. & Guggenheim, H. J. Magnetoelectric phenomena in BaMnF$_4$ and BaMn$_{0.99}$Co$_{0.01}$F$_4$. *Phys. Rev. B* **21**, 2926–2936 (1980).

41 Ederer, C. & Spaldin, N. A. Electric-field switchable magnets: The case of BaNiF$_4$. *Phys. Rev. B* **74**, 020401 (2006).

42 Brixner, L. H., Whitney, J. F., Zumsteg, F. C. & Jones, G. A. Ferroelasticity in LnNbO$_4$-type rare earth niobates. *Mater Res Bull* **12**, 17–24 (1977).

43 Yelissiyev, A. P. *et al.* Structures and optical properties of two phases of SrMgF$_4$. *Phys. Chem. Chem. Phys.* **17**, 500–508 (2015).

44 Setter, N. & Cross, L. E. The contribution of structural disorder to diffuse phase transitions in ferroelectrics. *J. Mater. Sci.* **15**, 2478–2482 (1980).

45 Salje, E. & Bismayer, U. Order parameter behaviour in the relaxor ferroelectric lead scandium tantalate. *J. Phys. Condens. Matter* **1**, 6967–6976 (1989).

46 Dawber, M., Rios, S., Scott, J. F., Zhang, Q. & Whatmore, R. W. Cryogenic studies of manganese-doped lead scandium tantalate: phase transitions or domain wall dynamics? *AIP Conf. Proc.* **582**, 1–10 (2001).

47 Siny, I. G., Katiyar, R. S. & Bhalla, A. S. Relaxor ferroelectrics. *Ferroelec Rev.* **2**, 51–76 (2000).

48 Oak, M. A. *et al.* 4d-5p orbital mixing and asymmetric In 4d-O 2p hybridization in InMnO$_3$: a new bonding mechanism for hexagonal ferroelectricity. *Phys. Rev. Lett.* **106**, 047601 (2011).

49 Huang, F. T. *et al.* Delicate balance between ferroelectricity and antiferroelectricity in hexagonal InMnO$_3$. *Phys. Rev. B* **87**, 184109 (2013).

50 Kumagai, Y. *et al.* Observation of persistent centrosymmetricity in the hexagonal manganite family. *Phys. Rev. B* **85**, 174422 (2012).

51 Mukherjee, S. *et al.* Room temperature nanoscale ferroelectricity in magneto-electric multiferroic thin films. *Phys. Rev. Lett.* **111**, 087601 (2013).

52 Singh, V., Mukherjee, S., Mitra, C. & Garg, A. Aging and memory effects in magnetoelectric gallium ferrite single crystals. *J. Magn. Magn. Mater.* **375**, 49–53 (2015).

53 Sun, Z. H., Zhou, Y. L., Dai, S. Y., Cao, L. Z. & Chen, Z. H. Preparation and properties of GaFeO$_3$ thin films grown at various oxygen pressures by pulsed laser deposition. *Appl. Phys. A* **91**, 97–100 (2008).

54 Song, S. *et al.* Multiferroic switching in GaFeO$_3$ films up to T = 400 K. *npj Asia Mater.* (in the press, 2015).

55 Sanchez, D. A., Ortega, N., Kumar, A., Katiyar, R. S. & Scott, J. F. Symmetries and multiferroic properties of novel room-temperature magnetoelectrics: Lead iron tantalite-lead zirconate titanate (PFT/PZT). *AIP Adv.* **1**, 042169 (2011).

56 Schiemer, J. *et al.* Studies of the room-temperature multiferroic Pb(Fe$_{0.5}$Ta$_{0.5}$)$_{0.4}$(Zr$_{0.53}$Ti$_{0.47}$)$_{0.6}$O$_3$: resonant ultrasound spectroscopy, dielectric, and magnetic phenomena. *Adv. Funct. Mater.* **24**, 2993–3002 (2014).

57 Evans, D. M. *et al.* Magnetic switching of ferroelectric domains at room temperature in a new Multiferroic. *Nat. Commun.* **4**, 1534–1540 (2013).

58 Gregg, J. M. *et al.* The nature of room-temperature magnetoelectric coupling in Pb(Zr,Ti)O$_3$-Pb(Fe,Ta)O$_3$. *Adv. Mat.* (in the press, 2015).

59 Kumar, A., Rivera, I., Katiyar, R. S. & Scott, J. F. Multiferroic Pb(Fe$_{0.66}$W$_{0.33}$)$_{0.80}$Ti$_{0.20}$O$_3$ thin films: room temperature relaxor ferroelectric and weak ferromagnetic. *Appl. Phys. Lett.* **92**, 132913 (2008).

60 Jonscher, A. K. Universal dielectric response. *Nature* **264**, 673–679 (1977).

61 Dielectric relaxation in solids. *J. Phys. D Appl. Phys.* **32**, R57–R70 (1999).

62 Kumar, A. *et al.* Magnetic control of large room temperature polarization. *J. Phys. Condens. Matter* **21**, 382204 (2009).

63 Pirč, R., Blinc, R. & Scott, J. F. Mesoscopic model of a system possessing both relaxor ferroelectric and relaxor ferromagnetic properties. *Phys. Rev. B* **72**, 214114 (2009).

64 Dawber, M., Jung, D. J. & Scott, J. F. Perimeter effect in very small ferroelectrics. *Appl. Phys. Lett.* **82**, 436–438 (2003).

65 Gruverman, A., Wu, D. & Scott, J. F. Piezoresponse force microscopy studies of switching behavior of ferroelectric capacitors on a 100-ns time scale. *Phys. Rev. Lett.* **100**, 097601 (2008).

66 Scott, J. F., Gruverman, A., Wu, D., Vrejoiu, I. & Alexe, M. Nanodomain faceting in ferroelectrics. *J. Phys. Condens. Matter* **20**, 425222 (2008).

67 Jiang, A. Q., Scott, J. F., Lu, H. B. & Chen, Z. Phase transitions and polarizations in epitaxial BaTiO3/SrTiO$_3$ superlattices studied by second-harmonic generation. *J. Appl. Phys.* **93**, 1180–1185 (2003).

68 Johnston, K., Huang, X., Neaton, J. B. & Rabe, K. M. First-principles study of symmetry lowering and polarization in BaTiO$_3$/SrTiO$_3$ superlattices with in-plane expansion. *Phys. Rev. B* **95**, 177601 (2004).

69 Gruverman, A. *et al.* Vortex Ferroelectric Domains. *J. Phys. Condens. Matter* **20**, 342201 (2008).

70 Schilling, A. *et al.* Domain structures in ferroelectric nanodots. *Nano Lett.* **9**, 3359–3364 (2009).

71 Baudry, L., Sene, A., Luk'yanchuk, I., Lahoche, L. & Scott, J. F. Polarization vortex domains induced by switching electric field in ferroelectric films with circular electrodes. *Phys. Rev. B* **90**, 024102 (2014).

72 Lukyanchuk, I. *et al.* High-symmetry polarization domains in low-symmetry ferroelectrics. *Nano Lett.* **14**, 6931–6935 (2014).

73 Scott, J. F. Cylinder stress in nanostructures: effect on domains in nanowires, nanotubes, and nano-disks. *J. Phys. Condens. Matter* **26**, 212202 (2014).

74 Lichtensteiger, C., Fernandez-Pena, S., Weymann, C., Zubko, P. & Triscone, J. M. Tuning of the depolarization field and nanodomain structure in ferroelectric thin films. *Nano Lett.* **14**, 4205–4212 (2014).

75 Dawber, M. & Bousquet, E. New developments in artificially layered ferroelectric oxide superlattices. *MRS Bull.* **38**, 1048–1055 (2013).

76 Rowley, S. E. *et al.* Ferroelectric quantum criticality. *Nat. Phys.* **10**, 367–372 (2014).

77 Rowley, S. E., Hadjimichael, M. & Scott, J. F. Quantum critical point in an organic ferroelectric. arXiv:1410.2908 (in the press, 2015).

78 Rowley, S. E. *et al.* Quantum Critical Point study in Multiferroic Hexaferrites: BaFe$_{12}$O$_{19}$, SrFe$_{12}$O$_{19}$, and PbFe3Ga9O19 -- Verification of the Khmelnitskii Theory. arxiv condmat:1507.01880 (2015).

79 Sushkov, O. P. in *Workshop on Topological Ferroelectrics* (eds Nagarajan V. & Seidel J.) Book of Abstracts (Sydney, Australia, 2015)

80 Chumakov, Y. M., Palomares-Sanchez, S. A., Guerrero-Serrano, A. L. & Martinez, J. R. Lattice vibration calculation of lanthanum hexaferrite. *Sci. J. SLP.* Article **2008**, 1SJ (2008).

81 Shneerson, V. L. & Khmelnitskii, D. E. Low-temperature displacement-type transition in crystals. *Sov. Phys. Solid State* **13**, 687–690 (1971).

82 Khmelnitskii, D. E & Shneerson, V. L. Phase-transition of displacement type in crystals at very low temperatures. *Zh. Eksp. Teor. Fiz.* **64**, 316–330 (1973).

83 Naumov, Il, Fu, H. X. & Bellaiche, L. Unusual phase transitions in ferroelectric nanodisks and nanorods. *Nature* **432**, 737–740 (2004).

84 Tang, Y. L. *et al.* Observrvation of a periodic array of flux-closure quadrants in strained ferroelectric PbTiO$_3$ films. *Science* **348**, 547–551 (2015).

85 Yadav, A. K. *et al.* Observation of Polar Vortices in Oxide Superlattices (in the press, 2015).

86 Piette, B. M. A. G., Kudryavtsev, A. & Zakrzewski, W. J. Skyrmions and domain walls in (2+1) dimensions. *Nonlinearity* **11**, 783–787 (1998).

87 Dawber, M., Gruverman, A. & Scott, J. F. Skyrmion model of nano-domain nucleation in ferroelectrics and ferromagnets. *J. Phys. Condens. Matter* **18**, L71–L75 (2006).

88 Cox, D. E., Shapiro, S. M., Cowley, R. A., Eibschutz, M. & Guggenheim, H. J. Magnetic and structural phase transitions in BaMnF$_4$. *Phys. Rev. B* **19**, 5754–5772 (1979).

89 Barthes-Regis, M. *et al.* Temperature dependence of the wave vector of the incommensurate modulation in two BaMnF$_4$ crystals grown by different technioques-neutron and x-ray measurements. *J. Physique. Lett.* **19**, L829–L835 (1983).

90 Levstik, A. *et al.* Dielectric study of the antiferrodistortive phase transition in BaMnF$_4$. *Ferroelectrics* **14**, 703–707 (1976).

91 Hidaka, M., Nakayama, T., Scott, J. F. & Storey, J. S. Piezoelectric resonance study of structural anomalies in BaMnF$_4$. *Phy. B* **133**, 1–9 (1985).

92 Cox, D. E. *et al.* X-ray diffraction and neutron measurements on BaMnF$_4$. *Phys. Rev. B* **28**, 1640–1643 (1983).

93 Scott, J. F. New results in Incommensurate crystals: Kink diffusion and long-period lock-in phases. *J. Raman Spectrosc.* **17**, 151–154 (1985).

94 Yamada, Y. & Hamaya, N. A unified view of incommensurate-commensurate phase transitions in A2BX4-type crystals. *J. Phys. Soc. Jpn.* **52**, 3466–3474 (1983).

95 Keeney, L. *et al.* Magnetic field-induced ferroelectric switching in multiferroic aurivillius phase thin films at room temperature. *J. Am. Ceram. Soc.* **96**, 2339–2357 (2013).

96 Feldkamp, G. E., Scott, J. F. & Windsch, W. Light-scattering study of phase transitions in ferroelectric tris-calcium chloride and its brominated isomorphs. *Ferroelectrics* **39**, 1163–1166 (1981).

97 Mackeviciute, R. *et al.* The perfect soft-mode: giant phonon instability in a ferroelectric. *J. Phys. Condens. Matter* **25**, 212201 (2013).

98 Jones, S. P. P. *et al.* Phase diagram and phase transitions in tris-sarcosine calcium chloride and its brominated isomorphs. *Phys. Rev. B* **83**, 094102 (2010).

99 Lashley, J. C. *et al.* Phase transitions in the brominated ferroelectric tris-sarcosine calcium chloride (TSCC). *Adv. Mater.* **26**, 3860–3866 (2014).

100 Bornarel, J. & Schmidt, V. H. Determination of Landau free-energy parameters by dielectric measurements in the ferroelectric TSCC. *J. Phys. C Solid State* **14**, 2017–2025 (1981).

101 Pawlowski, A. & Hilczer, B. Influence of lattice defects on the critical behavior of TGS single crystals. *Acta Phys. Polonca A* **56**, 639–643 (1979).

102 Scherwitzl, R. *et al.* Metal-insulator transition in ultrathin LaNiO$_3$ films. *Phys. Rev. Lett.* **106**, 246403 (2011).

103 Scott, J. F. in *Encyclopedia of applied physics* 14 (ed. Trigg G. L.) 497–506 (VCH: Berlin, Germany, 1983).

104 Qiu, S. L., Dutta, M., Cummins, H. Z., Wicksted, J. P. & Shapiro, S. M. Extension of the Lifshitz-point concept to 1st-Order phase transitions. *Phys. Rev. B* **34**, 7901 (1986).

105 Ishibashi, Y. & Hidaka, Y. On an isomorphous transition. *J. Phys. Soc. Jpn.* **60**, 1634–1637 (1991).

106 Marti, X. *et al.* Skin layer of BiFeO$_3$ single crystals. *Phys. Rev. Lett.* **106**, 236101 (2011).

107 Kumar, A., Scott, J. F., Martinez, R., Drinivasan, G. S. & Katiyar, R. S. In-plane dielectric and magnetoelectric studies of BiFeO$_3$. *Phys. Status Solidi A* **209**, 1207–1212 (2012).

108 Jarrier, R. *et al.* Surface phase transitions in BiFeO$_3$ below room temperature. *Phys. Rev. B* **85**, 184104 (2012).

109 Gurevich, V. L. & Tagantsev, A. K. Second sound in Ferroelectrics. *Ferroelec* **80**, 825–828 (1988).

110 Courtens, E., Hehlen, B., Farhi, E. & Tagantsev, A. K. Optic mode crossings and the low-temperature anomalies of SrTiO$_3$. *Zeitschrift für Physik B Condens. Matter* **104**, 641–642 (1997).

111 Salje, E. K. H., Aktas, O., Carpenter, M. A., Laguta, V. V. & Scott, J. F. Domains within domains and walls within walls: evidence for polar domains in cryogenic SrTiO$_3$. *Phys. Rev. Lett.* **111**, 247603 (2013).